JOURNAL OF MATERIALS SCIENCE: MATERIALS IN MEDICINE **16** (2005) 153–160

Dynamic creep and mechanical characteristics of SmartSet GHV bone cement

C. Z. LIU[1,2]*, S. M. GREEN[3], N. D. WATKINS[4], D. BAKER[4], A. W. MCCASKIE[2]
[1]*Northern Ireland Bioengineering Centre, University of Ulster, Newtownabbey BT37 0QB, Northern Ireland, UK*
[2]*Department of Trauma and Orthopaedic Surgery, University of Newcastle, Newcastle Upon Tyne NE2 4HH, UK*
E-mail: DES6CL@yahoo.com
[3]*Centre for Biomedical Engineering, University of Durham, Durham DH1 3LE, UK*
[4]*DePuy CMW, Blackpool FY4 4QQ, UK*

The restrained dynamic creep behaviour and mechanical properties of SmartSet GHV bone cement have been investigated at both room temperature and body temperature. It was found that the bone cement behaves significant differently at room temperature from that at body temperature. The test temperature had a strong effect on the creep performance of the bone cements with a higher creep rate observed at body temperature at each loading cycle. For both temperatures, two stages of creep were identified with a higher creep rate during early cycling followed by a steady state creep rate. The relationship between creep deformation and loading cycle can be expressed by a Hyperb 1 model. As a visco-elastic material, the sensitivity of bone cement to the temperature change was evident during mechanical testing. Compared to the mechanical strength at room temperature, a decreased value was demonstrated at body temperature. The bending modulus was very sensitive to the change in testing temperature, where a reduction of 52% was recorded. A significant reduction in compressive and bending strength, 31 and 23% were recorded respectively. The effect of temperature on bending strength was less apparent, where only 13% reduction was exhibited at body temperature compared to room temperature.

1. Introduction

Polymethylmethacrylate (PMMA) bone cement is commonly used in orthopaedic surgery. Several studies have evaluated the mechanical properties, creep behaviour, fatigue properties and fracture toughness of bone cement at room temperature [1–4]. However, some studies have suggested that the loosening of cemented total hip replacement (THR) is related to the cement performance in service [5–8]. A large number of studies reporting the mechanical properties of bone cement and the factors that affect these properties have been reported in the literature [1, 9–12]. When compared to the stress levels experienced in the cement mantle, the strength values found indicate that the bone cement is prone to fatigue fracture due to dynamic loading [13]. Acrylic bone cement at body temperature behaves in a manner that is neither that of a simple elastic solid, nor that of a true viscous liquid, it behaves as a visco-elastic solid [14].

Investigations on the creep of bone cement have resulted in mixed findings. Verdonschot *et al.* [15] reported that cement creep release cement stresses and creates a more favourable stress distribution at the bone cement-stem interface and at the bone-cement interface. Fowler *et al.* [16] postulated that metal-cement interface slip increases the long-term stability of a THR by protecting the cement-bone interface. Harris and colleagues [17] have stated that creep of the cement mantle surrounding a hip prosthesis may be negligible under cyclic physiological loading. Several investigators have studied the creep and relaxation behaviour of bone cement [18, 19], these studies revealed that creep strains could exceed the elastic ones. All these studies were performed on unconstrained cement specimens. However, *in vivo*, bone cement is restrained between the femoral component and the outside cortical bone and subjected to a dynamic loading cycle [20, 21]. SmartSet GHV bone cement is a newly launched bone cement, it is important to understand its dynamic creep behaviour and mechanical properties especially under environmental conditions similar to those experienced "*in-vivo*" such as temperature, restraint and loading cycle [14]. The authors have no intention to compare the

*Author to whom all correspondence should be addressed.

clinical performance of the SmartSet GHV with other bone cements.

2. Materials and experimental

2.1. Bone cement

Commercially available bone cement, SmartSet GHV (DePuy CMW, England), was used for the present study. Additionally, CMW1 radiopaque (DePuy CMW, England), Palacos R-40 (Heraeus Kulzer Gmbh, Germany) and Simplex P (Howmedica Int. Inc., Ireland) were also tested in the present study to allowed comparison with SmartSet GHV cement. All bone cements were two component system formed from an initial mixture of polymer powder and monomer liquid. CMW and Simplex P bone cement contained $BaSO_4$, whilst SmartSet GHV and Palacos R-40 contained ZrO_2 as radiopaque agent. The molecular weight distributions of the investigated bone cements are listed in Table I, and the powder particle size distributions are shown in Fig. 1

TABLE I Molecular weight distributions of bone cements (g mol^{-1})

Bone cement	SmartSet GHV	Simplex P	CMW1	Palacos R-40
Powder	1000000	107000	208905	945000
Matrix	549012	292600	872741	654463
Cured cement	756400	171000	444308	757300

2.2. Dynamic creep test

As hand mixing gives a better representation of the cement as it is in real life, in the present study, the test specimens were prepared by hand mixing one package (40 g powder, 20 ml liquid) at room temperature following the manufacturer's preparation procedure. The bone cement creep test specimen used was a hollow cylinder, with an inside diameter of 10 mm, outside diameter of 20 mm and 25 mm in length. This geometry was chosen to approximate that of the *in vivo* femoral component within cortical bone cavity to allow comparison with a cemented prosthesis in the femur. The hollow cylindrical mould cavities were filled once the mixed cement reached dough time. The bone cement was allowed to cure at room temperature in the moulds for 1 h, then specimens were removed from the moulds and cured in water at 37 °C for a period of 1 week before creep testing.

The creep test specimen and test jig used in this work has been reported elsewhere [20–23]. The specimen

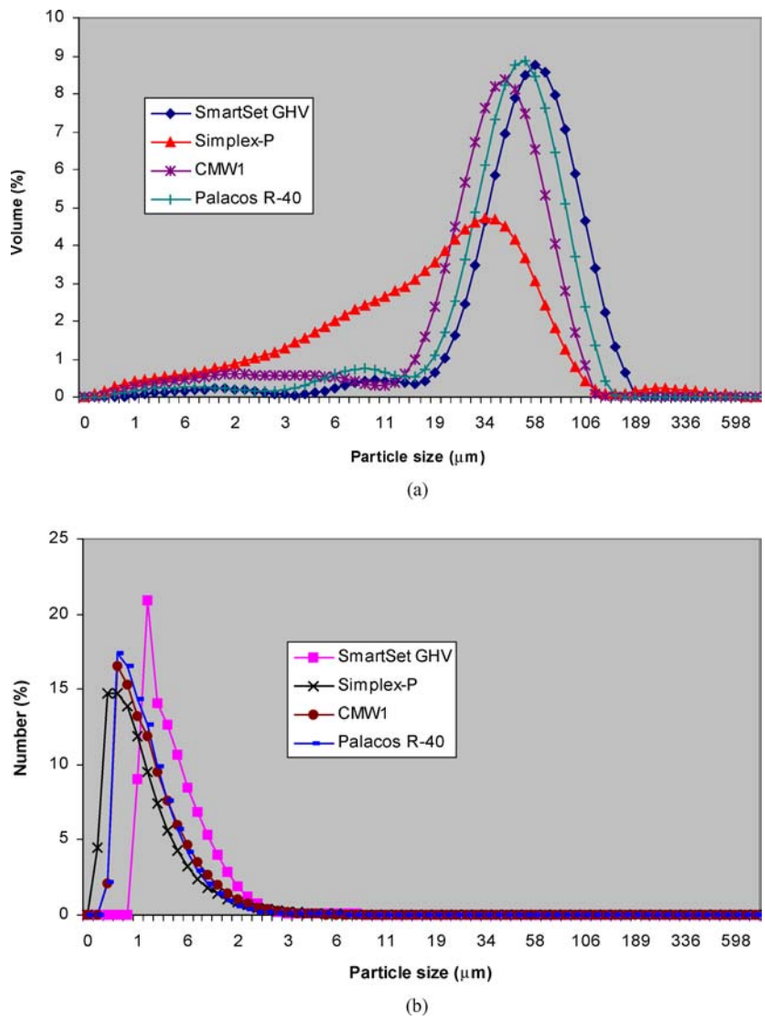

Figure 1 Particle size distributions of SmartSet GHV powder. The graphs show the practicle size distribution (a) by volume and (b) by number.

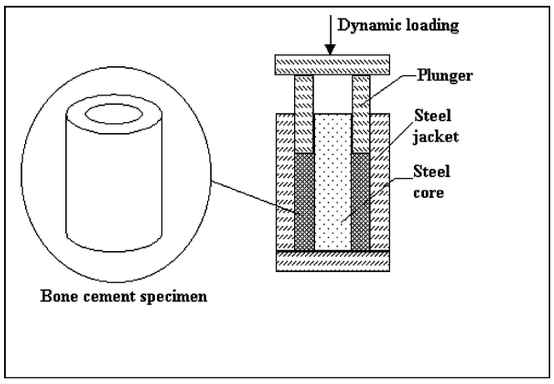

Figure 2 Creep test specimen and test rig.

was restrained between the external steel jacket and internal stainless steel core. A plunger, able to move up and down freely, was used to apply dynamic compressive load to the specimen, as shown in Fig. 2. The creep deformation of the specimens was measured using a micrometer with a resolution of 1 μm. The creep of the specimens, ε, was calculated use the following equation:

$$\varepsilon = \frac{L_o - L}{L_o} \times 100\% \quad (1)$$

where L_o is the original length of the specimen, L is the length after creep test.

Additionally, a semi-restrained creep test, i.e., the creep specimen restrained only by the internal core and un-restrained externally, was carried out to allow comparison with the clinical case of bone/cement interface failure.

The dynamic creep test was carried out on a modified Durham Mk. 2 hip joint simulator, as described elsewhere [21, 22, 24, 25]. The hip joint simulator uses a pneumatic actuator and proportional valve for each station. The signals used to control the force actuators produced a cyclic frequency of 1 Hz and a square wave loading cycle. The dynamic creep tests were conducted at both body and room temperatures. The compressive load level was set to 2500 N, giving an equivalent stress of 10.6 MPa, which is the stress level that a well-bonded stem may suffer *in vivo*.

2.3. Mechanical test and SEM examinations

Tensile, compressive and four point bending tests were performed using a Loyd 6000R universal testing machine at both room and body temperature, at a cross head speed of 5 mm min^{-1} for the bending and tensile test, and 25 mm min^{-1} for the compressive test. Follow the failure of the specimens upon mechanical testing, the specimens were examined by scanning electron microscopy (SEM) using a JEOL JSM-TC 848 apparatus operated at 20 kV, after sputtering a conductive gold film.

2.4. Particle size and molecular weight characterisations

The cement powder particle size distributions were analysed using a laser light scattering (LLS) particle size analyser (Masterizer, 2000, Malvern Instrument UK). The LLS technique is capable of quantifying particles lying within the size range of 0.05 to 1000 μm, which encompasses the reported range of cement particles. Dry cement powder was dispersed in water with the help of non-ionic surfactant (Nonidet, BDH) to make a dilute suspension. Within the instrument, the particles are suspended within a carrying fluid and circulated through an optical window placed in the path of a He-Ne laser beam. A passing particle causes diffraction of the laser beam, quantification of which enables calculation of the equivalent spherical volume of the particle using Mei theory.

For the molecular weight (Mw) determination, a small amount of cement powder/cement drilling debris was dissolved in chloroform. The sample was centrifuged to enable separation of the radio-pacifier. The solution was then decanted into a clean, dry separating funnel. The polymers were then re-precipitated by adding dropwise the filtrate into methanol. The re-precipitated polymer was then dried in a vacuum oven, dissolved in tetrahydrofuran, filtered and then injected into the gel permeation chromatography (GPC) to obtain chromatograph readings. The following equation was used to calculate the Mw of cement matrix (Mw(matrix)) formed from the liquid:

$$\text{Mw (cured)} = \frac{w_{\text{powder}} \times \text{Mw (powder)}}{w_{\text{powder}} + w_{\text{liquid}}} + \frac{w_{\text{liquid}} \times \text{MW (matrix)}}{w_{\text{powder}} + w_{\text{liquid}}} \quad (2)$$

Where Mw (cured) and Mw (powder) are the molecular weight of cured cement and cement powder respectively; w_{powder} and w_{liquid} are the weight of the cement powder excluding the radiopacifer and the liquid respectively.

3. Results

3.1. Creep behaviours

The creep variations of the specimens with the loading cycles at room and body temperature are shown in Fig. 3. This figure illustrates that the bone cement specimens demonstrate creep with respect to time.

It was observed that creep of the specimens increased with the loading cycles for both semi- and full-restrained specimens under both room and body temperatures. The fully restrained specimens demonstrated a very similar behaviour to that of semi-restrained specimens at room temperature (semi-restrained specimens demonstrated a slightly higher creep). Creep increased steadily with loading cycles during the tests, the total creep strains reached at after 5 million loading cycles were 0.4 and 0.36% for semi- and full-restrained specimens respectively. The very close creep strains between full and semi-restrained specimens indicated that restraint had no-significant effect on the creep of SmartSet GHV bone cements at room temperature.

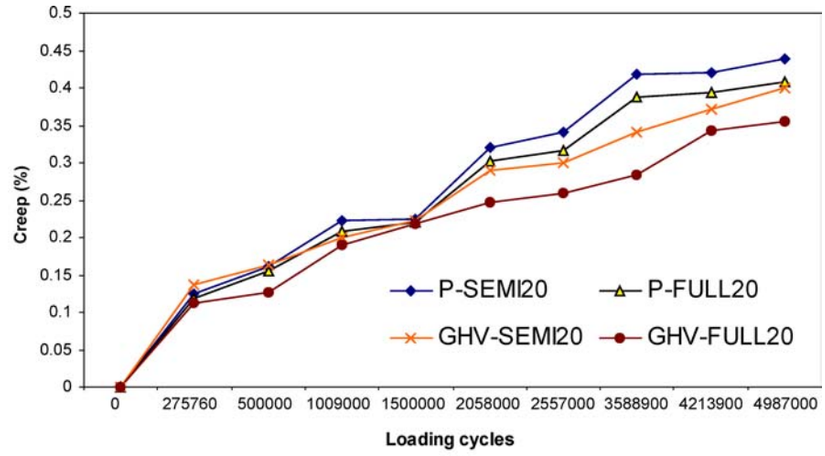

(a)

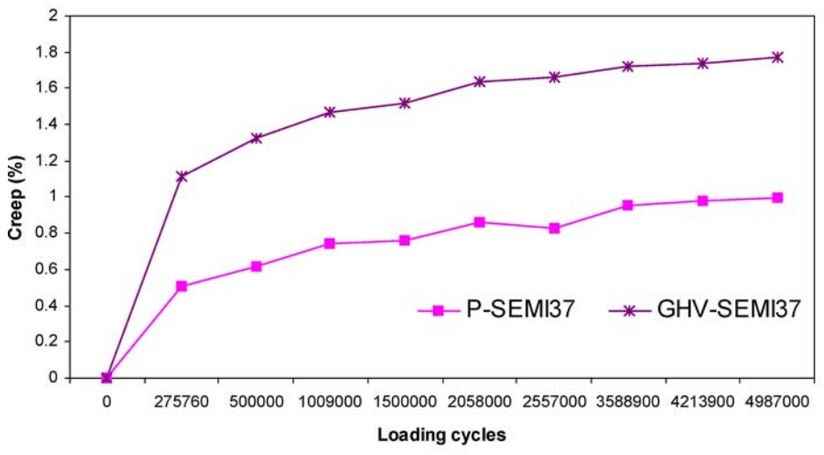

(b)

Figure 3 The creep variations with the loading cycles for SmartSet GHV and Simplex P bone cement: (a) tested at 20 °C and (b) tested at 37 °C.

A much higher creep strain was observed at body temperature than at room temperature at each loading cycle. Two creep stages are identified: a higher creep rate was measured during early cycling, followed by a levelling off creep stage at later cycling. The creep rate during early cycling was characterised by rapid increase of creep with loading cycles. This primary creep stage continued for about half million cycles. A creep strain of 1.33%, representing almost 75% of the total creep deformation for 5 million loading cycles, was reached at only 500000 loading cycles. Beyond that, the specimens creep further and thereafter levelled off. A similar tendency was also observed for the creep test at room temperature. After the initial creep stage, the creep rate of the specimens levelled off.

Conventional creep theories [26] suggested that the creep curves exhibit a linear relationship between time (t) and creep strain (ε) when considered on a double-logarithmic scale, i.e.

$$\log(\varepsilon) = b_0 \cdot \log(t) + b_1 \tag{3}$$

Verdonschot [18] measured the dynamic, compressive behaviour of surgical Simplex P acrylic bone cement, demonstrated that there was a linear relationship between the logarithmic values of the number of loading cycles and the creep strain. However, when this model was applied to the present experimental data, with time (t) being replaced by the number of loading cycles (N), it was found that this model did not fit well with the obtained data, especially for the initial creep. The regression analysis indicated that relationship between creep strain, ε, and the number of loading cycles, N, can be expressed by the following hyperb 1 model:

$$\varepsilon = \frac{P_1 \cdot N}{P_2 + N} \tag{4}$$

where P_1 and P_2 are constants. Application of the above model to the creep data sets, enabled the following relationships between creep strain and loading cycles to be determined.

For the semi-restrained SmartSet GHV specimens tested at body temperature, the following equation was obtained:

$$\varepsilon = \frac{1.787N}{180332 + N}, \quad R^2 = 0.99 \tag{5}$$

For semi-restrained SmartSet GHV bone cement tested at room temperature, the following equation was obtained:

$$\varepsilon = \frac{0.448N}{1063111 + N}, \quad R^2 = 0.96 \tag{6}$$

For the full-restrained SmartSet GHV tested at room temperature, the following equation was obtained:

$$\varepsilon = \frac{0.41N}{1184562 + N}, \quad R^2 = 0.97 \tag{7}$$

Statistical analysis indicated that the chi-square values given to the above each equation are less than the critical value $\chi^2_{(n=9,\,p=0.05)} = 16.92$, thus the null hypothesis was accepted and claim that the proposed model fit the experimental data very well [27].

3.2. Mechanical strength

The mechanical properties of SmartSet GHV bone cement are listed in Table II. It was observed that test temperature has a strong influence on the mechanical performance of the bone cement. A reduction in mechanical properties was generally demonstrated with increased testing temperature. The reductions of mechanical properties for specimen tested at body temperature compared to room temperature (expressed as a percentage) are also listed in Table II. It demonstrated that effect of the temperature varies for each mechanical property. The bending modulus was extremely sensitive to the change in testing temperature. A reduction of 52%, from 3517 MPa to 1684 MPa for bending modulus tested at room and body temperature respectively, was recorded. A significant reduction in compressive strength and bending strength were also recorded. The compressive strength reduced to 74 MPa from 107 MPa and bending strength reduced to 38 MPa from 50 MPa, which represent 31 and 23% reduction for compressive and bending strength respectively. Notable was the effect of temperature on bending strength, only 13% reduction was exhibited at body temperature compared to room temperature.

Compared with the reported mechanical properties of other bone cements [22, 28], such as CMW1, Simplex P and Palacos R-40 (Table II), it was found that SmartSet GHV has similar compressive and tensile strength to the other three bone cements. Analysis of variance (ANOVA) indicated that there was no significant difference between these bone cements [22]. However, SmartSet GHV and Palacos R exhibited bending modulus in the range of 3142–3517 MPa, which is higher than CMW1 and Simplex P bone cements' in the range of 2473–2837 MPa.

4. Discussion

Creep behaviour of hand-mixed bone cements, at several constant stress levels, has been investigated and demonstrated by Norman *et al.* [19] at room temperature. Their results indicated that creep strain after 24 h remained well below 1%. After 1000 h of a constant applied stress of 12.1 MPa, creep strain did not exceed 1%. They revealed that creep strain substantially increased at higher stress levels and increased non-linearly with increasing applied stress. Liu and Green *et al.* [23] reported the restrained dynamic creep behaviours of two clinical bone cements, Palacos R-40 and CMW1, at room temperature and body temperature, and found that the two cements demonstrated significantly different creep deformations, with Palacos R-40 bone cement demonstrating higher creep strain than CMW1 bone cement at each loading cycle. The test temperature had a strong effect on the creep performance of the bone cements with a higher creep rate observed at body temperature.

The creep phenomenon has been described as a stretching and re-aligning of molecular chains of acrylic bone cement. The ambient temperature has a significant effect on this process and high temperature facilitates the re-aligning of the molecular chains, resulting in high creep deformation. Lee *et al.* [14, 29] found in a series of tests designed to emulate the body's environment more closely that creep at 7 days was slower than at 2 days as expected. However, creep at 21 days and 42 days showed a reverse trend, with creep rates increasing. They concluded from their results that cement will creep at *in vivo* stress levels and that it is very sensitive to the ambient temperature and environment. As a visco-elastic material, the sensitivity of bone cement to the temperature change was evident during mechanical testing. Fig. 4 shows typical flexion curves of four point bending specimens with the loading. When tested at room temperature, the specimens fractured abruptly. The specimens become "ductile" when tested at body temperature, they did not fracture within the 15 mm deflection range of the test rig, but displayed a gradual, yielding mode.

The direct examination of the fracture surfaces of the samples in tensile testing revealed that all specimens exhibited "stress whitening", which may arise from the

TABLE II The mechanical properties of the investigated bone cement (MPa)

Temperature	Bone Cement	CS ± SD	TS ± SD	BS ± SD	BM ± SD
20 °C	SmartSet GHV	107.3 ± 3.3	50.2 ± 2.7	73.6 ± 9.9	3517 ± 159
	CMW1	114.7 ± 6.3	46.8 ± 3.8	81.7 ± 9.2	2473 ± 295
	Simplex P	102.1 ± 8.7	52.2 ± 2.7	76.5 ± 8.2	2837 ± 353
	Palacos R-40	101.1 ± 2.3	44.9 ± 3.3	70.5 ± 3.8	3142 ± 404
37 °C	SmartSet GHV	73.9 ± 2.8	38.4 ± 1.6	64 ± 2.3	1684 ± 36
Reduction percentage %		31	23	13	52

Note: CS: Compressive strength; TS: tensile strength; BT: four point bending strength; BM: bending modulus.

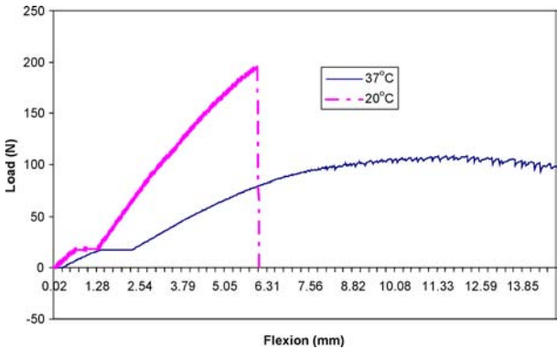

Figure 4 Four points bending test revealed an abrupt fracture mode for specimens at room temperature and gradual yielding mode at body temperature (the initial plateau at about 1 mm was caused by specimen micro-sliding within test rig).

development of craze before catastrophic crack propagation. The surfaces were fragmented by crevices and other cracks, as revealed in Fig 5. Detailed observation showed the samples fractured at body temperature had a rough topography. The appearance of delaminating material with the laminates fragmented under tensile stress and with more "in-depth" cracking resembles irregular stacks of plates or plateau, and "mountainous". It seemed there was extensive wafer drawing of thin layers of material, i.e. a typical ductile fractured behaviour [22]. Unlike samples fractured at body temperature, the samples fractured at room temperature demonstrated an irregular, flat texture surface, with more whitening signs, suggested a fast fracture behaviour. This confirmed the observation that the bone cement becomes ductile or less brittle at elevated temperature, as illustrated in Fig. 4.

Chemical compositions and micro-structure have influence on the mechanical behaviour of bone cement. Polymerisation of the liquid monomer gives rise to a polymer matrix that surrounds the pre-polymerised PMMA beads. Thus the performance of the matrix will have a strong influence on the mechanical behaviour of the cement. The molecular weight (Mw) of the interstitial matrix polymer for SmartSet GHV bone cement is lower than that of the pre-polymerised PMMA beads, as listed in Table I. Generally speaking, the Mw of a polymer influences the mechanical properties and physical properties such as hardness and rigidity [30]. Thus the matrix of the bone cement and interface between the matrix and the beads will determine the mechanical properties and time dependent properties. The difference in molecular weight between matrix and pre-polymerised beads and the presence of the ceramic radiopaque agent will result in a mis-match in elastic moduli and the generation of contact stresses at interfacial zone between matrix and beads, especially at elevated temperature. Under the action of dynamic loading, such as contact stresses, in addition to thermal stresses, could lead to beads partially debonding from the matrix. Micro-cracks would form and propagate, and these would eventually result in the early failure at body temperature, compared to the test at room temperature.

The main component in SmartSet GHV is methyl methacrylate-methylacrylate copolymer with a molecular weight of 1000000 g mol^{-1}. This results in a large PMMA beads compared with other clinical bone cements, such as CMW1 and Simplex P (Table I). As large PMMA beads possess less specific surface area than small beads (such as those found in CMW1 and Simplex P bone cement), this reduces the bead/matrix interfacial zone that transmits load from matrix to bead on dynamic loading. Reduced interfacial zone and contact areas are associated with higher interfacial stresses. When the interfacial stress exceeds the bonding strength between PMMA beads and matrix, the beads would debond from the matrix, and crevices will be produced, which will act as stress concentration sites. Cracks will propagate from these sites when specimens are subject to dynamic load, such as in the dynamic creep testing process, as revealed in Fig. 6. It is evident that most of the micro-cracks propagate around large PMMA beads, indicating a weak bonding between the large beads and the matrix. Fractography examination revealed features consistent with those seen by others investigators [31–33]. These included agglomeration of radiopaque agent and lack of bonding between radiopaque agent and surrounding matrix. The shrinkage during the curing process and difference in polymerisation between the beads and the matrix could induce interfacial stresses, weakening the bond between the beads and the matrix. Therefore,

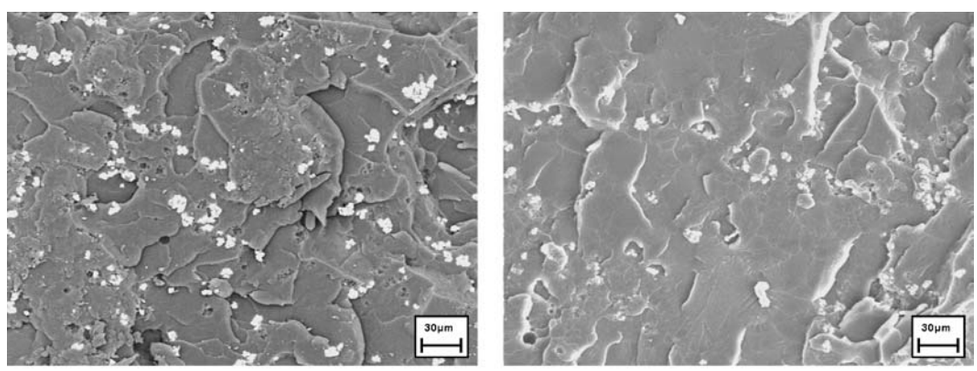

Figure 5 Tensile fractured topography for (a): 37 °C specimen; (b): 20 °C specimen.

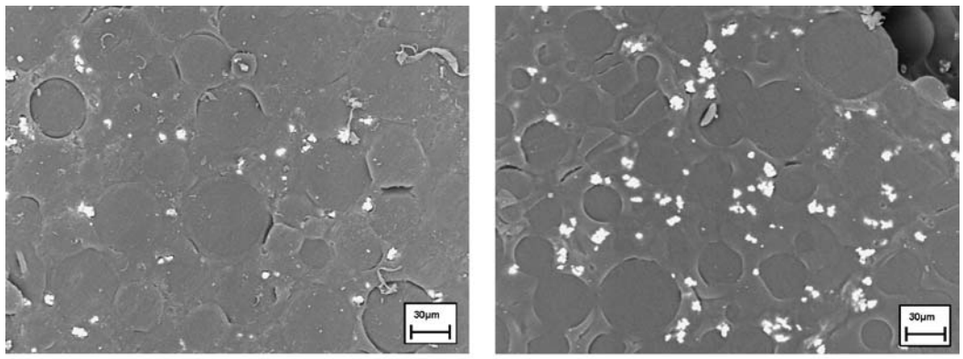

Figure 6 Crevice developed around large PMMA beads when subjected to dynamic loading cycles: (a) 37 °C specimen and (b) 20 °C specimen.

the micro-cracks propagate may preferentially around beads.

When mixed with the liquid component, the copolymer partly dissolves to form the polymethylmethacrylate matrix. The small PMMA beads have lower molecular weight thus the composition and structure is closer to that of the liquid monomer than large beads. Thus resulted a "good" compatibility between beads and matrix. This may be a factor in enhance the bonding strength between small beads and matrix in cement. At the same time, owing to the lower molecular weight, when contact with liquid, more portion of the smaller beads would swell and dissolve than the larger beads. The co-contribution of the higher compatibility and increased swelling and dissolution may be the reason why fewer crevices are found around small PMMA beads in bone cement, where as crevices were observed around large PMMA beads under the same loading conditions. However, this does not suggest that the cements with smaller bead size, low Mw are superior to the ones with larger bead size, as the performance of bone cement depends on many factors, especially compositions [4, 34].

In comparison with other on commercially available bone cements, it was found that SmartSet GHV is very close to Palacos R-40 bone cement in both mechanical and physical properties (Tables I and II). Both have a close particle size distribution. The molecular weight of SmartSet GHV and Palacos R are much higher than CMW1 and Simplex P cement (Table I), both for prepolymerised PMMA beads and cured cement. They have a lower molecular weight matrix than CMW1 but higher than Simplex P cement. In contrast to CMW1 and Simplex P bone cement, in which the powder has a lower molecular weight than the matrix, a notable decrease of molecular weight in cured cement was revealed in SmartSet GHV and Palacos R bone cement. Both SmartSet GHV and Palacos R demonstrated ductile behaviour, and sensitivity to the change in temperature, higher creep strain than CMW1 and Simplex P bone cement. The results observed here are in consistent with the results as reported by Harper and Bonfield [3]. As ductile bone cement, SmartSet GHV tends to creep more when subject to dynamic loading than a rigid or brittle bone cement. This was confirmed by the creep comparison between SmartSet GHV and Simplex P bone cement, as illustrated in Fig. 3. The SmartSet GHV creeps more than Simplex P bone cement at each loading cycles under the same test environment, especially at body temperature.

Several factors should be considered when interpreting the data. As a preliminary study on newly launched SmartSet GHV bone cement and the limitation of configuration of the hip joint simulator, the current study was carried out under dry conditions. Acrylic bone cement is a visco-elastic material, and thus creep strains are expected to depend upon environmental conditions. Moisture may have an important effect on the visco-elastic behaviour of bone cement, via the reported plasticization effect [29]. Under such conditions, bone cement may behave in a less rigid manner, and it is possible that fewer micro-cracks would have been produced in a more plasticised cement when subject to dynamic loading.

5. Conclusions

This study has shown that the test temperature had a strong effect on the creep performance and mechanical properties of the SmartSet GHV bone cement. At body temperature, the specimens become "ductile" and demonstrated significantly different from that at room temperature. Creep of the specimens at both temperatures (37 °C and 20 °C) increased with the loading cycles. Two stages, a higher creep rate during early cycles followed by a steady state creep stage, were identified which are hypothetically governed by two different creep mechanisms for SmartSet GHV bone cement. At body temperature, the bone cement demonstrated a much higher creep strain than at room temperature at each loading cycle. The relationship between the creep deformation and loading cycles can be expressed by a Hyperb 1 model.

The results have shown that the mechanical properties of the bone cement are also temperature dependent. A reduction in mechanical properties was generally demonstrated at body temperature, and the effect of the temperature varies for each mechanical property. The bending modulus was the most sensitive to the change of testing temperature, with a reduction of 52% was recorded. A significant reduction in compressive

strength and bending strength were also recorded, with a reduction of 31 and 23% respectively. Notable was the lower effect of temperature on bending strength, only 13% reduction was exhibited at body temperature compared to room temperature. Comparison with other bone cements suggested SmartSet GHV has a similar compressive and tensile strength to other commercial available bone cements.

Acknowledgments

Thanks are due to DePuy CMW for funding the present research and supplying the bone cements. The authors would like to acknowledge the help and support of Professor Anthony Unsworth at the Centre for Biomedical Engineering at University of Durham for his kind advice on the dynamic creep test of bone cements.

References

1. J. R. DE WIJN, T. J. J. H. SLOFF and F. C. M. DRIESSENS, *Acta. Orthop. Scand.* **46** (1975) 38.
2. J. P. DAVIES, D. O. O'CONNOR and J. A. GREER, *J. Biomed. Mater. Res.* **21** (1987) 719.
3. E. J. HARPER and W. BONFIELD, *ibid.* **53** (2000) 605.
4. C. Z. LIU, S. M. GREEN, N. D. WATKINS, P. J. GREGG and A. W. MCCASKIE, *Proceedings of the Institution of Mechanical Engineers, Part H: Journal of Engineering in Medicine* **215** (2001) 359.
5. Z. LU and H. MCKELLOP, *J. Biomed. Mater. Res.* **34** (1997) 221.
6. B. M. LWAK, O. K. LIM and Y. Y. KIM, *Intern. Orthop.* **2** (1979) 315.
7. R. T. MULLER, I. HEGER and M. OLDENBURY, *Archives of Orthop. and Trauma Surgery* **116** (1997) 41.
8. A. FAULKNER, L. G. KENNEDY, K. BAXTER, J. DONOVAN, M. WILKINSON and G. BEVAN, *Health Technology Assessment* **2** (1998) 1.
9. S. SAHA and S. PAL, *J. Biomed. Mater. Res.* **18** (1984) 435.
10. B. VAZQUEZ, S. DEB and W. BONFIELD, *J. Mater. Sci.: Mater. in Medicine* **8** (1997) 455.
11. E. LAUTENS and G. W. MARSHALL, *J. Biomed. Mater. Res.* **10** (1976) 837.
12. G. LEWIS, *J. Biomed. Mater. Res.* **40** (1999) 143.
13. R. HUISKES, *Current Orthop.* **7** (1993) 239.
14. A. J. C. LEE, R. D. PERKINS and R. S. M. LING, in "Implant Bone Interface" (Springer-Verlag, London, 1990) p. 85.
15. N. VERDONSCHOT and R. HUISKES, *Journal of Bone and Joint Surgery* **79-B** (1997) 665.
16. J. L. FOWLER, G. A. GIE and R. S. M. LING, *Orthop. Clin. North. Am.* **19** (1988) 477.
17. W. H. HARRIS, *Clin. Orthop. Rel. Res.* **274** (1992) 120.
18. N. VERDONSCHOT and R. HUISKES, *J. Biomed. Mater. Res.* **28** (1995) 575.
19. T. L. NORMAN, V. KISH, J. D. BLAHA, T. A. GRUEN and K. HUSTOSKY, *J. Biomed. Mater. Res.* **29** (1995) 495.
20. C. Z. LIU, S. M. GREEN, N. D. WATKINS, P. J. GREGG and A. W. MCCASKIE, in "The European Society for Biomaterials Conference (Barcelona, Spain, 2002) p. 276.
21. C. Z. LIU, S. M. GREEN, N. D. WATKINS, P. J. GREGG and A. W. MCCASKIE, *J. Mater. Sci. Lett.* **21** (2002) 959.
22. C. Z. LIU, in "Department of Trauma & Orthopaedic Surgery (University of Newcastle, Newcastle upon Tyne, United Kingdom, 2003) p. 286.
23. C. Z. LIU, S. M. GREEN, N. D. WATKINS, P. J. GREGG and A. W. MCCASKIE, *J. Mater. Sci.: Mater. Med.* **13** (2002) 1021.
24. C. Z. LIU, S. M. GREEN, T. J. JOYCE, P. J. GREGG and A. W. MCCASKIE, in "9th International Conference on Polymers in Medicine & Surgery (Krems, Austria) p. 397.
25. C. Z. LIU, S. M. GREEN, N. D. WATKINS, P. J. GREGG and A. W. MCCASKIE, in "European Society for Biomaterials 2001 Conference" (London, UK) p. P51.
26. D. J. CHWIRUT, *J. Biomed. Mater. Res.* **18** (1984) 25.
27. L. Q. REN, in "Book Experiment Design and Analysis" (Science and Technology Publishing Ltd of Jinlin Province, Changchun, P. R. China, 2001) p. 76.
28. C. Z. LIU, S. M. GREEN, N. D. WATKINS and A. W. MCCASKIE, *J. Mater. Sci. Lett.* **22** (2003) 709.
29. A. J. C. LEE, R. S. M. LING and S. S. VANGALA, *J. Med. Engng. Techn.* **2** (1977) 137.
30. S. A. VISSER, R. HERGENROTHER and S. L. COOPER, in "Biomaterials Science" (Academic Press, San Diego, California, USA, 1996) p. 105.
31. R. P. KUSY, *J. Biomed. Mater. Res.* **12** (1978) 271.
32. C. I. VALLO, *ibid.* **63** (2002) 226.
33. J. GRAHAM, L. PRUITT and M. RIES, *The Journal of Arthroplasty* **15** (2000) 1028.
34. C. Z. LIU, S. M. GREEN, N. D. WATKINS and A. W. MCCASKIE, in "Proceeding of 11th International Conference on Deformation, Yield and Fracture, of Polymers (Cambridge, UK, 2000) p. 325.

Received 7 October 2003
and accepted 1 July 2004